XXV Symposium *Vibrations in Physical Systems,* Poznan – Bedlewo, May 15-19, 2012

Dynamics of Mechanical Model of Implant-Tissue System in Ventral Hernia Repair

Izabela LUBOWIECKA
Gdansk University of Technology, ul. Narutowicza 11/1, 80-233 Gdansk, Poland
lubow@pg.gda.pl

Abstract

The paper deals with a finite element modelling of implants in the problem of ventral hernia repair. The synthetic mesh implanted in the abdomen during surgery is here modelled as a membrane structure. The system undergoes the internal abdominal pressure that occurs during the postoperative cough, the load identified in the literature as the main cause of the connection failure and hernia recurrence. The model can be used to estimate the forces appearing in the connections of tissue and implant for different materials of implants and different number of tacks. This can help to predict the fixing system, such as the number of tacks etc. to be provided during the surgery in order to resist the cough pressure and avoid the hernia recurrence. The dynamic analysis of the structure is compared to the laboratory experiments in a pressure chamber to demonstrate the accuracy of the proposed model.

Keywords: biomechanics, synthetic implant, membrane, dynamic analysis

1. Introduction

A hernia occurs when part of an internal organ protrudes through a weak area of muscle. Most hernias occur in the abdomen. Especially, the incisional hernias as large abdominal wall defects have been shown to have recurrence rates of between 25 to 52% when primarily repaired [1]. The usual treatment for a hernia is a repair surgery where the synthetic implants are fixed to the tissue called fascia in the human abdomen.

Even though the ventral hernia repair surgery is a common procedure, the mechanical properties of the tissue-implant system are unknown so the implantation of the repairing mesh depends on the surgeon knowledge and practice. Unfortunately, the recurrences of the illness still take place as shown e.g., in [2]. The number of the joints (called tacks) required for holding the implanted mesh correctly is undefined and their optimal position is only intuitive (Fig. 1). Moreover, the high number of joints can affect nerves and result in chronic pain, so the minimising of the tacks number standing the abdominal pressure is required.

For that, a mechanical model based on finite element method of implanted mesh is proposed here and its dynamic behaviour is studied to provide a methodology for the repair assessment. The model contains an orthotropic membrane structure of the material properties identified within the laboratory tests. The simple cable implant model of implanted mesh has been previously studied and presented in [3]. Also some attempts were undertaken to model implant behaviour as a membrane structure as shown in [4]. In addition a membrane model for a herniated rabbit abdominal wall with hernia orifice and implant was previously proposed and discussed in [5] but and any assessment method for the repair persistence was provided.

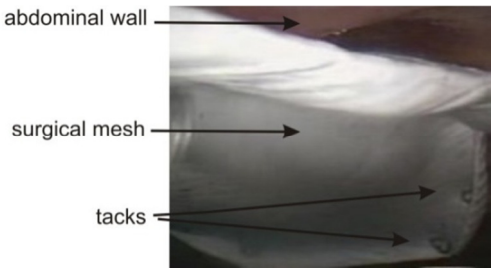

Figure 1. Hernia repair in human abdomen

The author pays considerable attention to the forces that appear in the connection between tissue and implant. These forces compared with the repair failure load identified in [6] are analysed to estimate the hernia repair persistence. For that reason, the mechanical model of whole abdomen is not necessary here. These forces should not exceed the experimental value of the strength of the tissue-implant connection that would mean that the hernia recurrence will not appear due to the appropriate load.

The finite element dynamic analysis of the system is performed and the results are compared to the laboratory tests on the implant-tissue system sample subjected to a pressure load in a specially prepared pressure chamber.

2. Mechanical model of implant. Materials and experimentation.

The surgical mesh Dual Mesh Gore® was taken to the analysis. Its material properties were identified on the basis of the one dimensional tensile tests on the machine Zwick Roel 020 as presented in [3-4] and [7-8].

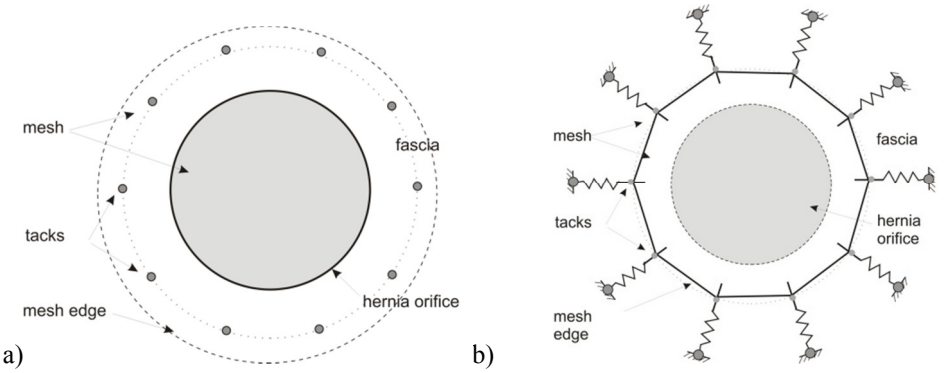

Figure 2. a) Scheme of repaired hernia; b) Implant model

The orthotropy of the surgical mesh material was observed as indicated in [9]. The material stiffness was described by bilinear elastic moduli $E_1 = 28.03$ N/mm and $E_2 = 25.54$ N/mm when the strain $\varepsilon \leq 0.3$ and $E_1 = 4.17$ N/mm and $E_2 = 2.84$ N/mm when $\varepsilon > 0.3$.

The model geometry (Fig. 2) refers to the clinical case of hernia with the 5 cm large orifice. As the common distance between joints differs from 2 to 4 cm, the largest as unfavourable one was considered in the model and also in the experiment. The membrane is a polygonal structure stretched out on 9 elastic supports every 4 cm, with 4 cm tissue overlap. This gives the membrane span equal to 0.12 m. The elastic supports, of the stiffness assuring the joints horizontal displacement observed within the experiment, represent the zone of interaction of the tissue and implanted membrane.

a) 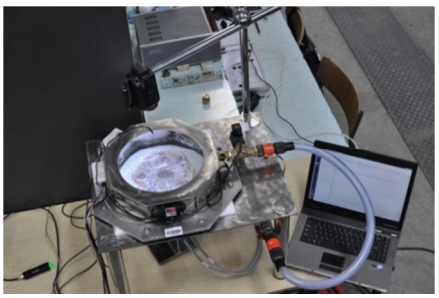 b) 

Figure 3. a) Experimental stand; b) Operated hernia specimen

The experiment was performed in a specially prepared pressure chamber where the air impact representing the cough pressure was applied to the specimen of implant fixed to the porcine tissue (Fig. 3). The pressure value was growing during 0.1 s until the value 270 mmHg identified in [10] as the cough pressure and then decreasing to 0 within next 0.1 s. The size and the fixing type referred to a real clinic case of hernia repair. The details of the experiments are presented in [8].

3. Finite element analysis and results

The nonlinear dynamic analysis was carried out by means of the MSC.Marc finite element commercial system. 469 (symmetric part) 4-node membrane element of type 18 (MSC.Marc) containing 3 translational degrees of freedom in each node was applied (see e.g. [11-12]), Fig. 4. The large strains and Total Lagrangean formulation were considered in the study. The implicit single step Houbolt algorithm (see e.g., [13]) was used to simulate the structure dynamics.

The dynamic analysis demonstrates relatively strong damping in the tissue-implant system, so the Rayleigh damping parameters were introduced also to the mechanical model. The parameters were estimated on the basis of modal analysis according to the formula (1)

$$\xi_i = \frac{\alpha}{2\omega_i} + \frac{\beta\omega_i}{2} \tag{1}$$

where α and β are respectively the mass and stiffness damping ω_i represents i-th natural frequency of the system [14]. For the tested implant, these two coefficients were

estimated as $\alpha = 2$ and $\beta = 0.01$, for which the simulation corresponds to the experi-experimental results.

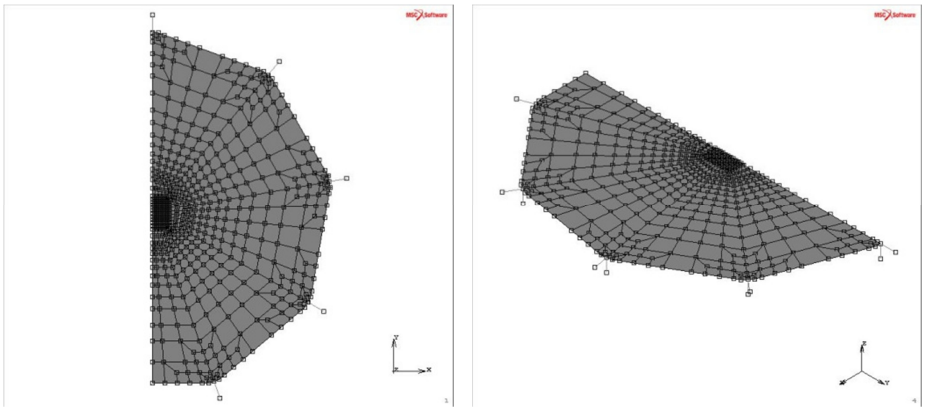

Figure 4. Finite element model of implant (symmetric part)

The dynamic analysis representing the experiment was conducted within the time of 2 s. The experimental and simulated results were compared on the example of the displacement functions.

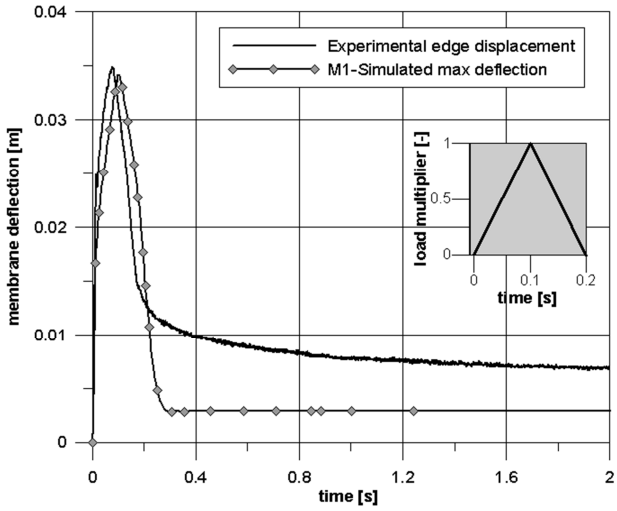

Figure 4. Dynamic analysis of the implanted mesh. Simulation vs. experiments

The registered and calculated values of the maximum deflection of the implant and the displacement of the hernia orifice are shown in Fig. 5. Relatively good accordance

between laboratory tests outcomes and the finite element analysis results means that the mechanical model can be applied for modelling of the tissue-implant behaviour.

The junction forces calculated in the points of tacks as the product of the spring stiffness and the tack displacement are used to the assessment of the repair persistence. In the studied case, these extreme forces are R_{max} = 2.25 N and R_{min} = 3 N respectively to the directions of the higher and lower elastic modulus E_1 and E_2 of the orthotropic implant. The difference between both forces is not very significant due to the fact that in this type of implant, the mechanical properties do not differ considerably. The maximum force does not exceed the limit identified for the tissue-implant connection identified in [6].

3. Conclusions

The author developed an orthotropic membrane model of a mesh implanted in a human body in the hernia repair surgery. The model can simulate the behaviour of the ventral hernia repair process under the intaabdominal pressure. The junction forces in the tacks points compared with the limit identified and documented in literature are used to estimate the repair persistence.

The proposed model behaviour matches accurately with the experiment. The maximum reaction forces achieved in this simulation and thus the largest expected values of the junction force in the tissue-implant system do not exceed the limit, what means that the repair should stand the cough pressure.

The presented solution can be applied to estimate the necessary joints number before the laparoscopic surgery when the synthetic implant is used in order to avoid the illness recurrences.

Even if the orthotropy of the implant is not strong, it is reflected in the reaction forces. This fact, together with the anisotropy of the human abdomen observed and described e.g., in [7] should be considered as clinic recommendations when planning the surgeries.

Acknowledgments

The Author wish to acknowledge prof. Czesław Szymczak, prof. Paweł Kłosowski and dr Agnieszka Tomaszewska their support of this contribution.

This study is partially supported by the EU, as part of the Innovative Economy Operational Programme (contract No UDA-POIG.01.03.01-22-086/08-00).

Computations were done in TASK Computer Science Centre, Gdańsk, Poland.

References

1. W.S. Cobb, J.M. Burns, R.D. Peindl, A.M. Carbonell, B.D. Matthews, K.W. Kercher, B.T. Heniford, *Textile Analysis of Heavy Weight, Mid-Weight, and Light Weight Polypropylene Mesh in a Porcine Ventral Hernia Mode,* Journal of Surgical Research, **136** (2006) 1–7, doi:10.1016/j.jss.2006.05.022.

2. C.R. Deeken, M.S. Abdo, M.M. Frisella, B.D. Matthews, *Physicomechanical evaluation of absorbable and nonabsorbable barrier composite meshes for laparoscopic ventral hernia repair*, Surg. Endosc. **212** (2011) 68-79.
3. C. Szymczak, I. Lubowiecka, A. Tomaszewska, M. Śmietański, *Modeling of the fascia-mesh system and sensitivity analysis of a junction force after a laparoscopic ventral hernia repair*, J. Theor. Appl. Mech. **48** (2010) 933-950.
4. I. Lubowiecka, C. Szymczak, A. Tomaszewska, M. Śmietański, *A FEM membrane model of human fascia-synthetic implant system in a case of a stiff ventral hernia orifice*, in: W. Pietraszkieiwcz, I. Kreja (Eds.), Shell Structures. Theory and Applications, CRC Press/Balkema, Londyn, 2010, pp. 311-314.
5. B. Hernandez-Gascon, E. Pena, H. Molero, G. Pascual, M. Doblare, M.P. Ginebra, J.M. Bellon, B. Calvo, *Mechanical behaviour of synthetic surgical mesh: Finite element simulation of th ehernia ab-dominal wall*, Acta Biomatrialia, **7** (2011) 3905-3913.
6. M. Śmietański, J. Bigda, K. Iwan, M. Kołodziejczyk, J. Krajewski, I. Śmietańska, P. Gumiela, K. Bury, S. Bielecki, Z. Śledziński, *Assessment of usefulness of different tacks in laparoscopic ventral hernia repair (IPOM),* Surg. Endosc. **21** (2007) 925-928.
7. C. Szymczak, I. Lubowiecka, A. Tomaszewska, M. Śmietański: *Investigation of abdomen surface deformation due to life excitation: implications for implant selection and orientation in laparoscopic ventral hernia repair.* Clinical Biomechanics, **27** (2012) 105-110.
8. I. Lubowiecka, A. Tomaszewska, C.Szymczak, B. Meronk, M. Śmietański, *Modelling and experimental study of implants used In laparoscopic hernia repair*, in: Proceedings of Nowe Kierunki Rozwoju Mechaniki, Hucisko 2011, Poland (in Polish).
9. E. R. Saberski, S. B. Orenstein, Y. W. Novitsky, *Anisotropic evaluation of synthetic surgical meshes*, Hernia **15** (2011) 47-52.
10. Z.J. Twardowski, R. Khanna, K.D. Nolph, *Intransabdominal pressures during natural activities in pa-tients treated with CAPD*, Nephron, **44** (1986) 129-135.
11. A.P.S. Selvadurai, *Deflections of a rubber membrane*, J. Mech. Phys. Solids, **54** (2006) 1093-1119.
12. D.C. Pamplona, P.B. Goncalves, S.R.X. Lopes, *Finite deformations of cylindrical membrane under internal pressure*, Int. Journal of Mechanical Sciences **48** (2006), 683-696.
13. K. Subbaraj, M.A. Dokainish, *A survey of direct time-integration methods in computational structural dynamics – II. Implicit Methods*, Compt. Struct. **32** (1989) 1387-1401.
14. M. Liu, D.G. Gorman, *Formulation of Rayleigh damping and its extensions*, Compt. Struct. **57** (1995) 277-285.

XXV Symposium *Vibrations in Physical Systems,* Poznan – Bedlewo, May 15-19, 2012

Numerical Aeroacoustic Research of Transmission Loss Characteristics Change of Selected Helicoidal Resonators due to Different Air Flow Velocities

Wojciech ŁAPKA
Poznań University of Technology, Institute of Applied Mechanics
Jan Paweł II 24, 60-965 Poznań, Poland, wojciech.lapka@put.poznan.pl

Abstract

This paper presents the results of aeroacoustic numerical simulations for three types of helicoidal resonators placed inside straight cylindrical duct. The same ratio $s/d = 1.976$ is considered for three numbers of helicoidal turns $n = 0.671$, $n = 0.695$ and $n = 1.0$. Also three types of transmission loss characteristics are represented. Three-dimensional models were calculated by the use of a finite element method in Comsol Multiphysics Acoustics Module – Aeroacoustics with flow, Frequency Domain. The change of transmission loss characteristics of helicoidal resonators is presented for different air flow velocities in the range from 1 m/s to 20 m/s for cylindrical duct of diameter $d = 0.125$m.

Keywords: helicoidal resonator, sound attenuation, aeroacoustics.

1. Introduction

Speed of a main flow of air inside ducted system can affect on acoustical properties of applied there passive noise control devices [7,8]. Stronger influence could be observed for resonators. As it has already been well described [3-6], by using helicoidal resonators in ducted systems one can obtain numbers of acoustic resonances inside helicoidal profile, which results in sound reduction at the systems outlet. Also this paper takes under consideration the first approach of solving the problem of helicoidal resonators acoustic attenuation characteristic change due to assuming different speed of a main flow of air inside a straight cylindrical duct. Investigated in this paper models of helicoidal resonators are presented in Fig. 1, where s denotes the length of one helicoidal turn.

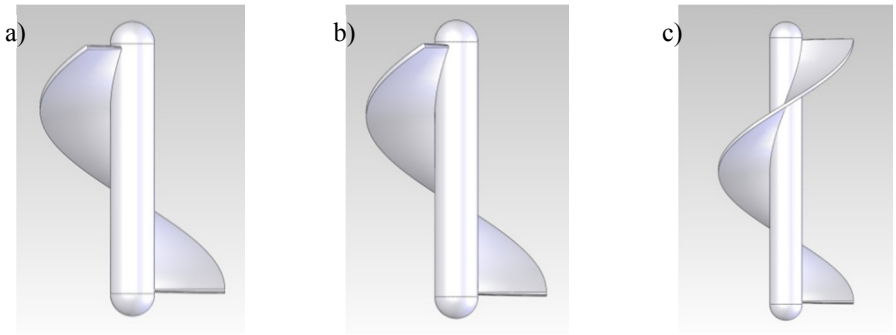

Figure 1. Helicoidal resonators with ratio $s/d = 1.976$ and number of helicoidal turns $n = 0.671$ (a), $n = 0.695$ (b), $n = 1.0$ (c)

Helicoidal resonators consist of a central axis mandrel with ratio $d_m/d = 0.24$, where d_m denotes the diameter of mandrel, and d is the diameter of cylindrical duct. Helicoidal profile has the ratio $g/d = 0.024$, where g denotes the thickness of helicoidal profile. The cylindrical duct diameter $d = 0.125$ m. Small difference for two selected helicoidal resonators in number of turns $n = 0.671$ and $n = 0.695$ results from representation of two different acoustic attenuation characteristics obtained in previous work [6], which are presented in Fig. 2 and Fig. 3, respectively.

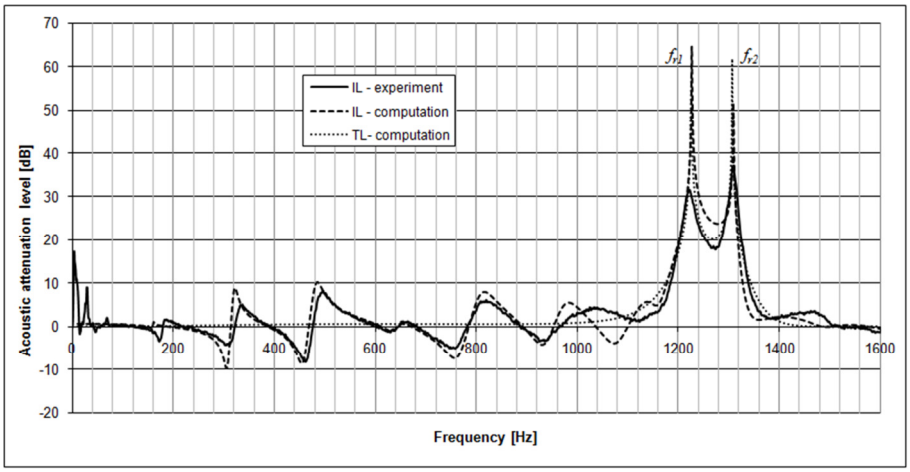

Figure 2. Acoustic attenuation performance parameters levels for helicoidal resonator inside pipe ($d = 0.125$ m) with the number of turns $n = 0.671$ [6]

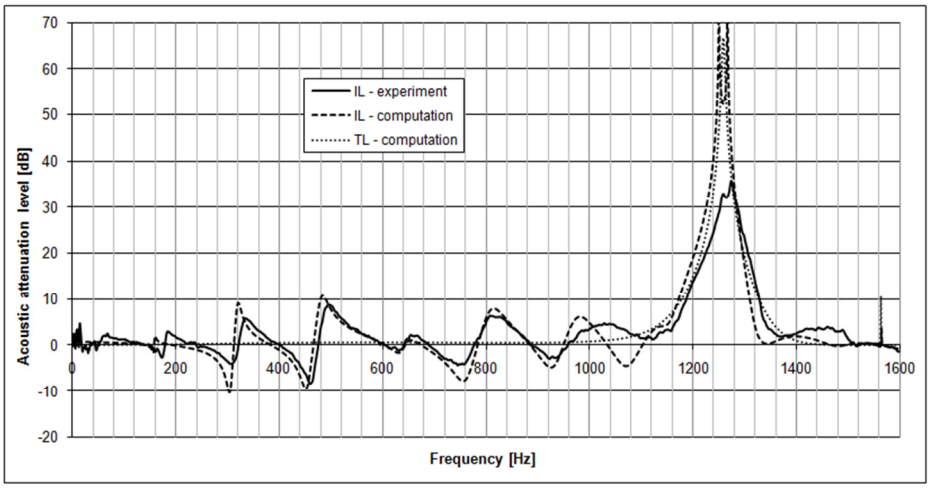

Figure 3. Acoustic attenuation performance parameters levels for helicoidal resonator inside pipe ($d = 0.125$ m) with the number of turns $n = 0.695$ [6]

In Figs. 2 and 3 are presented comparisons between two acoustic attenuation performance parameters, Insertion Loss (IL) and Transmission Loss (TL), obtained in numerical computations (computation) and experimentally (experiment) [6].

2. Basic Characteristics of Numerical Aeroacoustic Simulations

Three-dimensional models were calculated by the use of finite element method in Comsol Multiphysics Acoustics Module – Aeroacoustics with flow, Frequency Domain [1]. Schematic view of investigated cylindrical duct with helicoidal resonator is presented in Fig. 4.

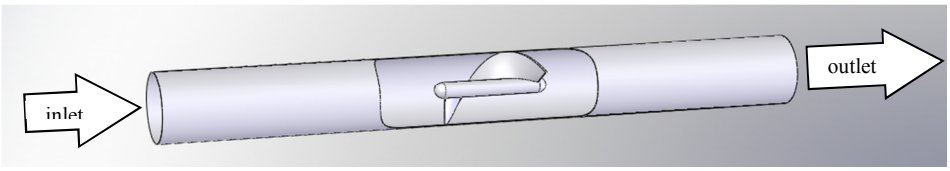

Figure 4. Schematic view of investigated cylindrical duct with helicoidal resonator

To solve aeroacoustic problem in COMSOL flow is assumed to be compressible, inviscid, barotropic, and irrotational [1]. In this paper, for investigated velocities of air flow in range from 1 m/s to 20 m/s, the Reynolds number varies from Re~8333 to Re~166670, respectively. In that case the turbulent flow should be considered [2], but due to fact that COMSOL can solve only CFD turbulent flow without acoustic, the aeroacoustics was used as a weak solution for coupling acoustic with flow, in this case. Also obtained in this paper results can strongly differ from real results, but the aim of this work is to obtain an overview of helicoidal resonators transmission loss change due to different velocities of air flow.

As an acoustical attenuation performance parameter is used the transmission loss (TL) [1, 3-5, 7, 8], which is obtained by integrating the incident nominal acoustic pressures squared at the inlet (*w_in*) and actual transmitted acoustic pressures squared at the outlet (*w_out*) all anechoically terminated, and solving equation:

$$TL = 10\log(w\_in/w\_out), \text{ dB} \tag{1}$$

Boundary conditions are described as in COMSOL Multiphysics [1]:

- hard boundary condition - all surfaces of cylindrical duct and helicoidal resonators are hard,
- slip velocity equals zero at all surfaces of cylindrical duct and helicoidal resonators,
- normal flow at the outlet equals zero,
- mass flow at the inlet varies from 1 m/s to 20 m/s,
- plane wave radiation - at the inlet and outlet, while at the inlet the velocity potential equals 1 m^2/s.

Finite element mesh is automatically generated as a free tetrahedral and controlled by physics. The stationary solver is used.

3. Results

In Fig. 5, Fig. 6 and Fig. 7 are presented transmission loss characteristics of helicoidal resonators with $s/d = 1.976$ and $n = 1.0$, $n = 0.695$ and $n = 0.671$, respectively, for different velocities of air flow. Results are presented in the range of frequency from 1200 Hz to 1350 Hz, which is the specific frequency range for investigated models.

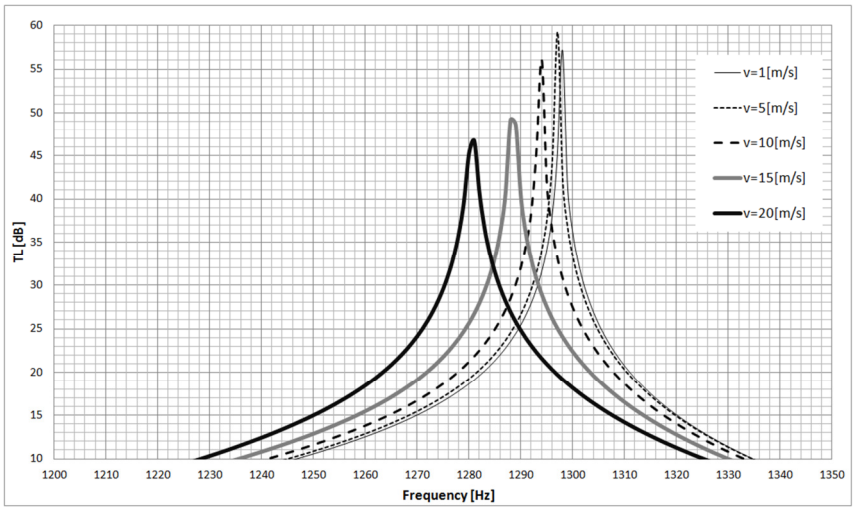

Figure 5. Transmission loss characteristics for helicoidal resonator with $s/d = 1.976$ and $n = 1.0$ for different velocity of air flow v

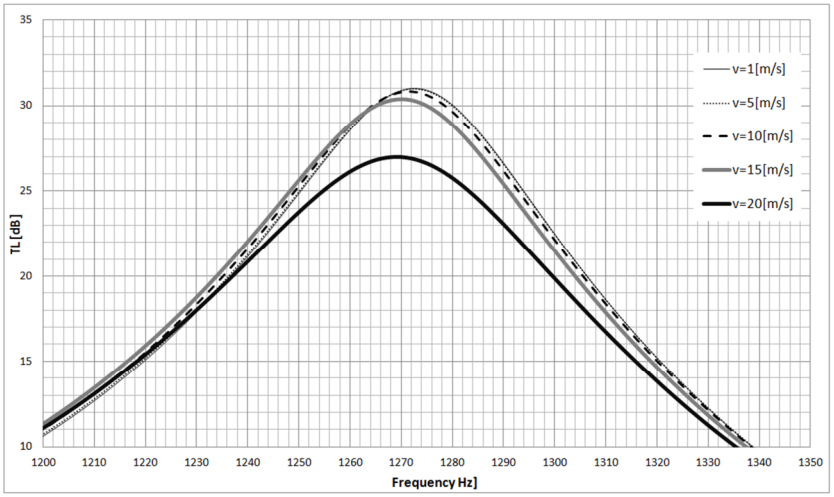

Figure 6. Transmission loss characteristics for helicoidal resonator with $s/d = 1.976$ and $n = 0.695$ for different velocity of air flow v [m/s]

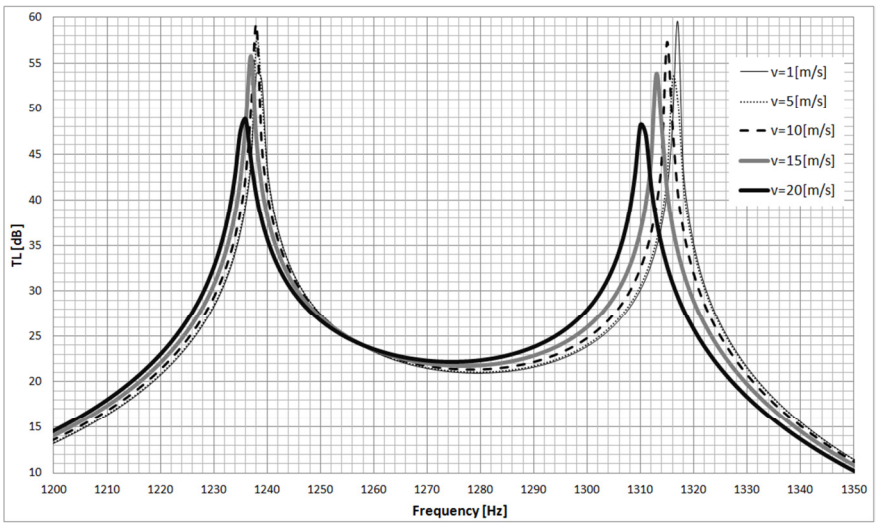

Figure 7. Transmission loss characteristics for helicoidal resonator with s/d = 1.976 and n = 0.671 for different velocity of air flow v [m/s]

4. Conclusions

In general, for investigated helicoidal resonators, when the velocity of air flow becomes greater the resonance frequencies as well as TL levels become lower.

For helicoidal resonator with n = 1.0 can be observed the biggest frequency difference between velocities v = 1 m/s and v = 20 m/s and it equals about 18 Hz. TL level reduces in this case for about 10 dB.

However, for helicoidal resonator with n = 0.695 in frequency domain can be observed small difference, which equals about 4 Hz, and similar small difference for TL levels which equals about 5 dB.

For helicoidal resonator with n = 0.671 can be observed bigger change for the second resonance frequency, which equals about 7 Hz, than for the first resonance frequency, where the difference equals only about 2 Hz. In this case the reduction of TL levels is similar for both frequencies and it equals about 10 dB. Here interesting is fact, that for the lowest TL level between resonance frequencies, which equals about 21 dB for v = 1-5 m/s, it increases for about 1 dB for v = 20 m/s.

Globally, up to 5 m/s of air flow velocity inside ducted system the resonance frequency does not change. Also, when applying helicoidal resonators for typical ventilation system, where the velocity of main air flow varies up to 5 m/s, there is no need to include any velocity corrections. But for higher velocities, typically in industrial applications, there should take place some air velocity corrections.

In this paper, the obtained numerical results can strongly differ from real results, but the aim of this work was to obtain an overview of helicoidal resonators transmission loss change due to different velocity of air flow, which was here realized. Hence, the

experimental researches of the influence of air flow velocity on acoustic attenuation characteristics change of helicoidal resonators should give the exact results.

Acknowledgments

The author gratefully acknowledges the funding by the Polish Ministry of Science and Higher Education in the years 2010-2013 as a research project N N502 4557 39.

References

1. COMSOL Multiphysics version 4.2.a, *Acoustic Module, User's Guide and Model Library Documentation Set*, COMSOL AB, www.comsol.com, Stockholm, Sweden, (2011).
2. Jeżowiecka-Kabsch K., Szewczyk H., *Mechanika płynów*, Oficyna Wydawnicza Politechniki Wrocławskiej, Wrocław, (2001) 386.
3. Łapka W, *Acoustic attenuation performance of a round silencer with the spiral duct at the inlet*, Archives of Acoustics, **32** (2007) 247-252.
4. Łapka W., *Acoustical properties of helicoid as an element of silencers*, Doctoral work, Faculty of Mechanical Engineering and Management, Poznań University of Technology (2009).
5. Łapka W., *Helicoidal resonator*, Proceedings of 39th International Congress and Exposition on Noise Control Engineering INTER-NOISE 2010, 9 pages in CD-ROM, Lisbon, Portugal, (2010) 9 pages in CD-ROM
6. Łapka W., Cempel C., *Acoustic short helicoidal resonator-computational and experimental investigations*, Proceedings of 58th Open Seminar on Acoustics, OSA 2011, Gdańsk-Jurata, Poland, (2011) 9-16.
7. Munjal M. L., *Acoustics of Ducts and Mufflers with Application to Exhaust and Ventilation System Design*, Inc., Calgary, Canada, John Wiley & Sons, (1987) 328.
8. Ver I. L., Beranek L. L., *Noise and vibration control engineering*, 2nd edition, Hoboken, John Wiley & Sons, Inc., New Jersey, USA, (2006) 966.